Available online at www.sciencedirect.com
ScienceDirect
Mendeleev Commun., 2010, **20**, 12–14
Mendeleev Communications

Impedance spectroscopy study of lithium ion diffusion in a new cathode material based on vanadium pentoxide

Dmitry A. Semenenko,[a] Tatiana L. Kulova,[b] Alexander M. Skundin,[b] Daniil M. Itkis,[a] Ekaterina A. Pomerantseva,*[a] Eugene A. Goodilin[a,c] and Yuri D. Tretyakov[a,c]

[a] *Department of Materials Science, M. V. Lomonosov Moscow State University, 119991 Moscow, Russian Federation. Fax: +7 495 939 0998; e-mail: pomeran@inorg.chem.msu.ru*
[b] *A. N. Frumkin Institute of Physical Chemistry and Electrochemistry, Russian Academy of Sciences, 119991 Moscow, Russian Federation*
[c] *Department of Chemistry, M. V. Lomonosov Moscow State University, 119991 Moscow, Russian Federation*

DOI: 10.1016/j.mencom.2010.01.005

The high discharge capacity (*ca.* 380 mAh g^{-1} in the first cycle) and diffusion coefficients of Li^+ ranging from ~10^{-10} to ~10^{-9} cm^2 s^{-1} were estimated from electrochemical experiments for the new composite material based on vanadium pentoxide xerogel and carbon nanotubes synthesized using freeze-drying technology demonstrating that it can be used in cathodes for advanced lithium-ion batteries.

The development of Li-ion rechargeable batteries ushered in the wireless revolution and spreading of the portable electronic devices; it has also stimulated a quest for batteries to power hybrid electric and all-electric vehicles. The future use of electrical energy depends on the development of the next generation of high-power, high-capacity and high-energy batteries. In particular, search for new cathode materials is essentially needed. Vanadium oxides are among the best positive electrode materials for rechargeable lithium-ion batteries, due to their high intercalation voltage and large specific capacity. Different forms of vanadium pentoxide have been obtained, *i.e.*, crystalline V_2O_5, xerogels,[1–3] aerogels,[4,5] nanocomposites with conductive polymers[6–8] and nanostructured materials (nanotubes, nanorods and nanoparticles).[9,10] Note that a discharge capacity of $V_2O_5{\cdot}nH_2O$ aerogel (~600 mAh g^{-1}) is several times higher than the capacity of a commercially used $LiCoO_2$ cathode.[11] Another family of vanadium pentoxide-based materials are nanocomposites with conductive polymers[8] and carbon nanotubes (CNT).[12,13] Interestingly, the V_2O_5/single-wall carbon nanotubes (SWCNT) composite has shown much better performance than that obtained with polyaniline (PANI), in terms of both specific capacity and capacity retention.[13] The comparison between nanocomposites of V_2O_5 with carbon black (CB) and SWCNT showed that the traditional composite with CB particles forms aggregates, which may occlude the vanadium oxide surface.[13] In the case of V_2O_5/SWCNT nanocomposites, vanadium oxide ribbons interweave with nanotubes and in spite of intimate contact between two components an electrolyte can freely access vanadium oxide surface that leads to enhanced properties.[13]

Semenenko *et al.*[14] demonstrated that the electrochemical properties of V_2O_5 freeze-dried xerogel are much better in comparison with the xerogel dried in conventional way. Water evaporation is much faster during a vacuum freeze-drying process than for thermal evaporation, resulting in the formation of an amorphous distorted structure with high specific surface area. Thermal analysis data indicated that freeze-dried xerogel contained 14.4–17.2 wt% water corresponding to the formula $V_2O_5{\cdot}nH_2O$ (n = 1.7–2.1). Discharge capacity of the material at the first cycle was 240 mAh g^{-1} and irreversible capacity loss did not exceed 5 mAh g^{-1}. This value corresponds to intercalation of 1.6 lithium atoms per formula unit, while vanadium mean oxidation number changes from +5.0 to +4.2.[14]

One of the major problems limiting the manufacture of vanadium oxide-based rechargeable lithium batteries is fast degradation of the active cathode material during lithium cycling. As a result, even after a few intercalation/deintercalation cycles, a significant capacity fading is often observed. Diffusion of lithium ions in a solid material is one of the processes stipulating the mechanism of charge accumulation. Thus, the estimation of diffusion parameters can help to elucidate the nature of material degradation and give ideas on the material stabilization for a long-term use.

Here, we report for the first time on the impedance spectroscopy study of lithium diffusion in the freeze-dried V_2O_5 xerogel/CNT composite.[†]

Figure 1(*a*) shows the microstructure of a freeze-dried V_2O_5 xerogel/CNT composite material. Pure freeze-dried xerogel appears as a yellow-green soft fibrous substance;[14] while a composite material has a typical black colour. As it was demonstrated previously,[12,13] in the case of V_2O_5/CNT composites, the intimate contact between two components and high electric conductivity due to the homogeneous distribution of a conductive component (CNT), which has the similar to the V_5O_5 nanoribbons mor-

[†] The V_2O_5 gel was synthesized using the ion-exchange technique described elsewhere.[1] The gel was frozen in liquid nitrogen and dried in FREEZONE 6 lyophilizer (Labconco) for two days. Thus obtained material was kept in a vacuum at 240 °C (higher temperatures lead to crystallization of water-free V_2O_5).[1,3]

The V_2O_5/CNT composite was prepared by mixing a water-ethanol suspension of carbon nanotubes (Aldrich, technical grade) with isopolyvanadic acid solution that contained growing polymeric chains (the solution used was aged after ion exchange for 2 min only to stop oxolation process). The mixture was sonicated for 15 min in an ultrasonic bath, freeze-dried and then kept under vacuum and high temperature using the conditions described above.

Micromorphology study was performed using a Supra 50 VP scanning electron microscope (LEO).

Experimental details on galvanostatic lithium intercalation/extraction and cycling voltammetry are given in the Online Supplementary Materials.

Impedance spectroscopy measurements were performed using a 1255B frequency response analyzer (Solartron analytical) in a frequency range from 10^{-1} to 10^6 Hz and an amplitude of 10 mV. The equilibrium state was achieved by keeping a positive electrode (~10 mg) for 1000 s at each potential. Raw data were analyzed using the ZView-Impedance Software (Scribner Associates).

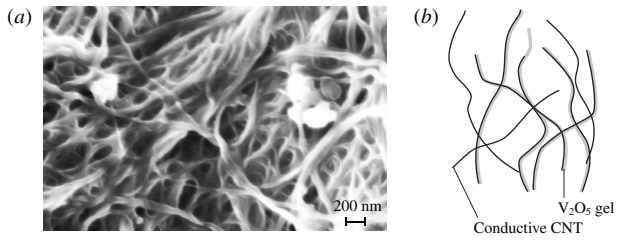

Figure 1 $V_2O_5{\cdot}nH_2O$ xerogel/carbon nanotubes composite material synthesized using cryochemical technology: (*a*) SEM image, (*b*) scheme of formation.

phology and dimensional scale, results in the improved electrochemical performance of the cell. During the composite synthesis V_2O_5 ribbons grow and interweave with CNT [Figure 1(*b*)] forming a porous material with high specific surface area and facilitated access to the electrolyte.

Figure 2(*a*) displays a typical Nyquist plot of the ac-impedance measured at different lithium intercalation levels and after the complete discharge at certain cycles (1 and 100) for V_2O_5/CNT composite. In general, each impedance spectrum consists of a depressed arc in the high-frequency region and a straight line inclined at a constant angle at low frequencies. Experimental ac-impedance spectra were fitted according to the model proposed elsewhere.[15] This model suggests that the cathode material is composed as follows [see Figure 2(*b*)]: particles of an active material ($V_2O_5{\cdot}nH_2O$ xerogel) are covered with a passive film and an interfacial electrical double layer (EDL). The particles of active material are randomly connected with the particles of conductive additive, which in our case is CNT shown however as globules in Figure 2(*b*) for visual simplicity. The model[15] describes a depressed semicircle as a combination of two semicircles with diameters corresponding to the dynamic resistivity

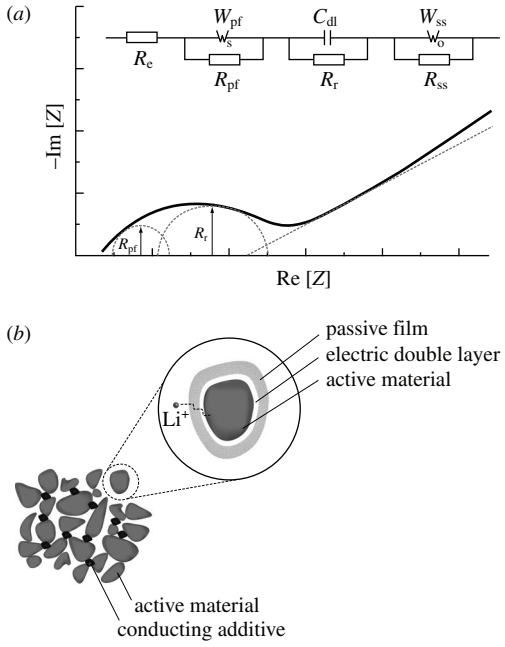

Figure 2 (*a*) Typical view of the impedance spectra measured for the three-electrode cell containing V_2O_5/carbon nanotubes composite material and (*b*) a schematic view of the cathode material. Areas corresponding to the different processes at the active part of the electrode and constituting the equivalent circuit (shown in the inset) are indicated: R_e is the non-active component of the resistivity (including resistivity of electrolyte, resistivity of secondary charge carriers transfer, *etc.*), R_{pf} is the resistivity of the passive film bypassed by the diffusion (W_{pf}), R_r is the resistivity of the lithium intercalation reaction into the active electrode material bypassed by the double layer capacity (C_{dl}), R_{ss} and W_{ss} are the resistive and Warburg impedance elements corresponding to the diffusion deep into the bulk of the material.

of passive film (R_{pf}) in parallel with Warburg diffusion corresponding to the diffusion through passive film (W_{pf}) and a resistivity of lithium electrochemical intercalation into an active material (R_r) and associative EDL capacity (C_{edl}) [Figure 2(*a*)]. Solid state diffusion of lithium ions into the bulk of the active cathode material is represented by Warburg impedance element (W_{ss}) with a resistive part (R_{ss}). In this study, the possible equivalent circuit was proposed in the inset of Figure 2(*a*).

Resistivity of the intercalation reaction (R_r) and resistivity of the passive film (R_{pf}) were estimated for electrodes with different discharge states (different levels of intercalated lithium ions). Figure 3 shows the cyclic voltammogram (CV) of the $V_2O_5{\cdot}nH_2O$ xerogel cathode. The cathodic part of CV displays four peaks of lithium intercalation at 3.36, 3.16, 2.51 and 2.26 V, while in the anodic part of CV three lithium extraction peaks are observed at 3.46, 3.24 and 2.65 V, while a broad maximum at 2.65 V most probably consists of two superimposed peaks at 2.79 and 2.60 V. Experimental ac-impedance spectra were measured at potentials that were chosen as the mean values between corresponding cathodic and anodic peaks (3.42, 3.20, 2.65 and 2.43 V). The difference between potential values of cathodic and corresponding anodic peaks (~100–300 mV) is typical of intercalation materials and caused by delayed (not instant) lithium ions diffusion into the material. The slight material degradation is related to the incomplete lithium ions extraction from the positions corresponding to the CV peaks at low potentials, which can be due to the severe structure distortions upon lithium intercalation. However, the use of ultra-fine materials results in improved cyclic performance because of shorter diffusion distances and reduced internal tension emerging in the material during lithium intercalation.

The evolution of diffusion parameters was monitored by measuring the ac-impedance spectra after 100 lithium intercalation/deintercalation cycles at the same polarization potentials. The efficiency of lithium intercalation in different positions after long-term cycling of the cathode was estimated by calculation of R_r values after 100 charge/discharge cycles.

The Nyquist plots of ac-impedance for V_2O_5/CNT composite electrode measured at different potentials in the first discharge cycle are shown in Figure 4(*a*), while Figure 4(*b*) demonstrates impedance spectra at 3.20 V polarization potential after 1st and 100th cycles of lithium intercalation/deintercalation. The summary of equivalent circuit parameters estimated by fitting of experimental impedance spectra using least square method is presented in Table 1 (see Online Supplementary Materials). Following the data reported,[16] we suggested that the double layer is ~0.5–0.7 nm thick and its thickness does not change significantly with the lithium intercalation degree. Thus, the capacity of the double layer (C_{dl}) has to be ~10^{-4} F (Table 1, Online Supplementary

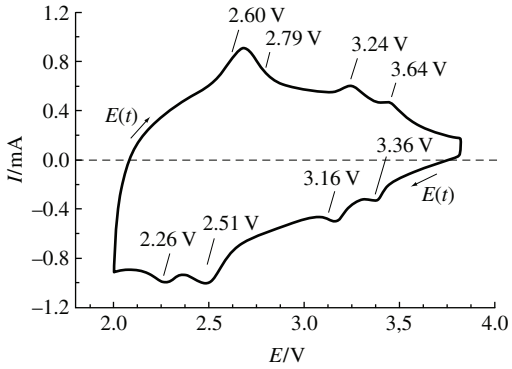

Figure 3 Cyclic voltammogram of $V_2O_5{\cdot}nH_2O$ xerogel electrode cycled between 2.0 and 3.8 V at a scan rate of 0.13 mV s^{-1} (1st cycle). Electrolyte is 1 M $LiClO_4$ in PC:DME (7:3). Lithium insertion/extraction potentials are indicated.

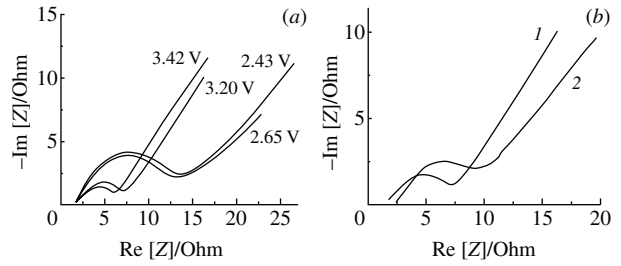

Figure 4 Experimental impedance spectra measured for the tree-electrode cell containing (*a*) original V_2O_5/carbon nanotubes composite material discharged to different potential values, (*b*) (*1*) original composite material and (*2*) the same material after 100 cycles discharged to the potential of 3.20 V. The frequencies of the semicircle maxima are ~150–175 Hz for all impedance spectra.

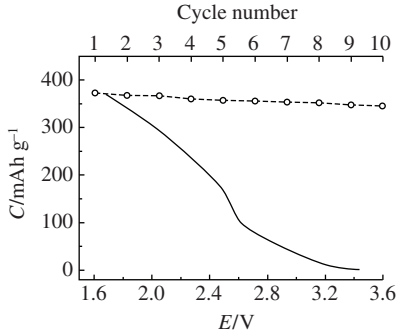

Figure 5 Discharge curve of $V_2O_5 \cdot nH_2O$ xerogel/carbon nanotubes composite electrode (1st cycle) and capacity retention for the first ten cycles. Electrolyte is 1 M $LiClO_4$ in PC:DME (7:3).

Materials). On the other hand, the capacity of the passive film is about ten times higher,[16] which was also taken into account during fitting (Table 1, Online Supplementary Materials).

The intercalation reaction resistivity increases with the potential becoming more negative which corresponds to a larger amount of lithium intercalated in the active material. After a long cycling the dependence of reaction resistivity (R_r^{100}) on the amount of intercalated lithium is less pronounced than after the first cycle (R_r^1). Deep lithium intercalation, as well as long cycling (Figure 4), results in the growth of passive film and consequently in the increase of R_{pf} resistivity (Figure 2).

Effective lithium diffusion coefficient was calculated as follows:

$$D_{eff} = (dE/dQ)^2/2\rho^2w^2; \quad (1)$$

$$w^2 = 2\pi f(-\mathrm{Im}\ z)^2, \quad (2)$$

where D_{eff} is the effective diffusion coefficient, dE/dQ is the derivative of potential in respect to a charge passed, ρ is the X-ray density of the active material (4–5 g cm^{-3} for vanadium oxides), w is the Warburg function, Im z is the reactance at a linear part of line corresponding to Warburg impedance [see Figure 2(*a*)], f is the frequency at the same point. The Warburg function in equation (1) assumes semi-infinite diffusion model implying that the particles size should be of the order of 50–100 μm. However, here we consider effective diffusion, while the term 'effective' means that the ions transfer under the experimental conditions not only occurs due to diffusion, but is also generated by electrical force. It corresponds to the charge transfer in the solid material, as a whole, between points of potential application, rather than in a single particle. Thus, the particles size of the order of < 100 nm shown in the SEM micrograph [Figure 1(*a*)] is in agreement with the proposed model.

The value of dE/dQ was estimated from quasi-equilibrium discharge experiments performed with V_2O_5/CNT composite electrodes (Figure 5). At the first dicharging, the composite electrodes showed a capacity of ~380 mAh g^{-1} which is 1.5 times higher than the capacity of the similarly obtained V_2O_5 xerogel (however, without vacuum drying and with AB conductive additive instead of CNT).[14] After ten lithium intercalation/deintercalation cycles discharge capacity of V_2O_5/CNT composite electrode was about 330 mAh g^{-1} that is ~87% of the initial value (Figure 5).

The estimated effective diffusion coeffcients for V_2O_5/CNT composite electrode material at the first cycle are 2×10^{-10}–5×10^{-9} and 3×10^{-10}–3×10^{-9} cm^2 s^{-1} after long cycling. The lithium diffusion coefficients in V_2O_5 xerogels have been reported[17] to be in the range of 10^{-8}–10^{-17} cm^2 s^{-1}. In addition, it was shown that the mobility ot Li^+ ions decreases with the growth of the amount of intercalated lithium ions as a result of Li^+–Li^+ interaction.[2] Thus, the lithium diffusion coefficients characteristic of V_2O_5/CNT composite electrode prepared in this work are similar to the best values for the same class of materials.[17] Therefore, V_2O_5/CNT composites are considered as promising cathode materials for a new generation of rechargeable lithium cells.

In conslusion, the synthetic approach based on polymerization of vanadia around carbon nanotubes and freeze-drying of the thus obtained gels is considered as an effective way to prepare composite electrode materials with enhanced electrochemical characteristics. The discharge capacity of V_2O_5/CNT composite electrode at the first cycle is ~380 mAh g^{-1}, and it remains at a relatively high level during further lithium cycling. The lithium diffusion coefficients estimated from impedance spectroscopy data are rather high and could be compared to the highest lithium diffusion coefficients typical of the same class of materials.

This work was supported by the Russian Foundation for Basic Research (grant no. 07-03-00749) and the Russian Federal Agency of Science and Innovations (contract no. 02.513.12.3016).

Online Supplementary Materials

Supplementary data associated with this article can be found in the online version at doi:10.1016/j.mencom.2010.01.005.

References

1 J. Livage, *Chem. Mater.*, 1991, **3**, 578.
2 F. Huguenin and R. M. Torresi, *J. Braz. Chem. Soc.*, 2003, **14**, 536.
3 G. S. Zakharova and V. L. Volkov, *Usp. Khim.*, 2003, **72**, 346 (*Russ. Chem. Rev.*, 2003, **72**, 311).
4 H. P. Wong, B. C. Dave, F. Leroux, J. Harreld, B. Dunn and L. F. Nazar, *J. Mater. Chem.*, 1998, **8**, 1019.
5 D. B. Le, S. Passerini, J. Guo, J. Ressler, B. B. Owens and W. H. Smyrl, *J. Electrochem. Soc.*, 1996, **143**, 2099.
6 G. R. Goward, F. Leroux and L. F. Nazar, *Electrochim. Acta*, 1998, **43**, 1307.
7 I. Boyano, M. Bengoechea, I. de Meatza, O. Miguel, I. Cantero, E. Ochoteco, J. Rodriguez, M. Lira-Cantu and P. Gomez-Romero, *J. Power Sources*, 2007, **166**, 471.
8 E. A. Ponzio, T. M. Benedetti and R. M. Torresi, *Electrochim. Acta*, 2007, **52**, 4419.
9 G. S. Zakharova, V. L. Volkov, V. V. Ivanovskaya and A. L. Ivanovskii, *Usp. Khim.*, 2005, **74**, 651 (*Russ. Chem. Rev.*, 2005, **74**, 587).
10 A. V. Grigorieva, T. L. Kulova, A. M. Skundin, E. A. Goodilin, A. V. Garshev and Yu. D. Tretyakov, *J. Altern. Energy Ecol.*, 2008, no. 8, 86.
11 M. S. Whittingham, *Chem. Rev.*, 2004, **104**, 4271.
12 W. Dong, J. Sakamoto and B. Dunn, *J. Sol-Gel Sci. Technol.*, 2003, **25**, 641.
13 F. F. C. Bazito and R. M. Torresi, *J. Braz. Chem. Soc.*, 2006, **17**, 627.
14 D. A. Semenenko, T. L. Kulova, A. M. Skundin, M. G. Kozlova, E. A. Pomerantseva, A. V. Grigorieva, E. A. Goodilin and Yu. D. Tretyakov, *J. Altern. Energy Ecol.*, 2007, no. 4, 83.
15 M. D. Levi and D. Aurbach, *Electrochim. Acta*, 1999, **45**, 167.
16 J. Zhou and P. H. L. Notten, *J. Power Sources*, 2008, **177**, 553.
17 F. Huguenin and R. M. Torresi, *J. Phys. Chem. C*, 2008, **112**, 2202.

Received: 3rd April 2009; Com. 09/3314